

Clear Signature of the (2×1) Reconstruction of Calcite $(10\bar{1}4)$ Jens Schütte,[†] Philipp Rahe,[†] Lutz Tröger,[‡] Sebastian Rode,[†] Ralf Bechstein,^{‡,§} Michael Reichling,[‡]
and Angelika Kühnle^{*,†}[†]Institut für Physikalische Chemie, Johannes Gutenberg-Universität Mainz, Jakob-Welder-Weg 11, 55099 Mainz, Germany, and [‡]Fachbereich Physik, Universität Osnabrück, Barbarastr. 7, 49076 Osnabrück, Germany.[§]Present address: Interdisciplinary Nanoscience Center (iNANO), Department of Physics and Astronomy, Aarhus University, Ny Munkegade, DK-8000 Aarhus C, Denmark.

Received December 14, 2009. Revised Manuscript Received January 24, 2010

Calcite is a mineral of fundamental importance that plays a crucial role in many fields of research such as biomineralization, biomolecule adsorption, and reactivity as well as industrial and daily life applications. Consequently, the most stable cleavage plane of calcite has been studied extensively using both direct imaging techniques such as atomic force microscopy as well as spectroscopic and diffraction techniques. Several surface structures have been reported for the $(10\bar{1}4)$ cleavage plane of calcite differing from the simple bulk-truncated structure and an ongoing controversy exists in literature whether the cleavage plane exhibits a (2×1) reconstruction or not. We study the $(10\bar{1}4)$ cleavage plane using high-resolution noncontact atomic force microscopy (NC-AFM) under ultrahigh vacuum conditions and obtain a clear signature of the (2×1) reconstruction. This reconstruction is observed in very narrow tip–surface distance ranges only, explaining why in some experiments the reconstruction has been observed and in others not. Moreover, as all sample preparation is performed in ultrahigh vacuum, the possibility of the (2×1) reconstruction being adsorbate-induced appears rather unlikely. Additionally, tip-induced surface changes are ruled out as origin for the observed reconstruction either. In conclusion, our study suggests that the (2×1) reconstruction is a true surface property of the $(10\bar{1}4)$ cleavage plane of calcite.

Introduction

Calcite, the most stable polymorph of CaCO_3 , is one of the most abundant simple salts in nature. Calcite formation is governed by the presence of biological macromolecules, resulting in biominerals with outstanding properties.^{1,2} Calcite has been discussed as a possible origin for the homochirality of life as the adsorption of amino acids has been demonstrated to be enantio-specific on the $(10\bar{1}4)$ cleavage plane of calcite.^{1–3} More than 40% of the known oil resources are estimated to be stored in calcite-containing rocks.⁴ Furthermore, calcite is used in many industrial products such as paints, paper chemicals, cement as well as cosmetics and pharmaceuticals.⁵ Because of its birefringence,⁶ high-purity calcite is used in optical devices. On the other hand, calcite precipitation upon scaling is usually undesired in industrial and daily life applications such as water desalination and laundry and, thus, avoided by addition of suitable polyelectrolytes.^{7,8}

Being the most abundant face of calcite, the $(10\bar{1}4)$ cleavage plane of calcite has been studied extensively using surface sensitive analysis techniques including low-energy electron diffraction

(LEED),⁹ X-ray photoelectron spectroscopy (XPS),⁹ and atomic force microscopy (AFM).^{10–18} Most AFM investigations were performed in liquid environment and focused on the dissolution and growth of calcite depending on the ionic strength and pH value,^{19–24} however, an increasing number of studies has recently been dedicated to clarifying whether the cleavage plane resembles the bulk-truncated structure or exhibits a surface reconstruction.^{9,14,18,25} Despite these efforts, a comprehensive understanding of the atomic-scale structure is still lacking, and the issue of possible surface reconstructions remains inconclusive.

Calcite crystallizes in a trigonal crystal system ($\bar{3}2/m$) and belongs to the space group $R\bar{3}c$.²⁶ Calcite can be described with

(11) Sand, K. K.; Stipp, S. L. S.; Hassenkam, T.; Yang, M.; Cooke, D.; Makovicky, E. *Mineral. Mag.* **2008**, *72*, 353–357.

(12) Jin, M. X.; Shimada, E.; Ikuma, Y. *J. Ceram. Soc. Jpn.* **1999**, *107*, 1166–1170.

(13) Foster, A.; Shluger, A.; Barth, C.; Reichling, M., Contrast Mechanisms on Insulating Surface. In *Noncontact Atomic Force Microscopy*; Morita, S., Wiesendanger, R., Meyer, E., Eds.; Springer: Berlin, 2002.

(14) Liang, Y.; Lea, A. S.; Baer, D. R.; Engelhard, M. H. *Surf. Sci.* **1996**, *351*, 172–182.

(15) Ohnesorge, F.; Binnig, G. *Science* **1993**, *260*(5113), 1451–1456.

(16) Rachlin, A. L.; Henderson, G. S.; Goh, M. C. *Am. Mineral.* **1992**, *77*, 904–910.

(17) Rode, S.; Oyabu, N.; Kobayashi, K.; Yamada, H.; Kühnle, A. *Langmuir* **2009**, *25*, 2850–2853.

(18) Stipp, S. L. S.; Eggleston, C. M.; Nielsen, B. S. *Geochim. Cosmochim. Acta* **1994**, *58*, 3023–3033.

(19) Baltrusaitis, J.; Grassian, V. H. *Surf. Sci.* **2009**, *603*, L99–L104.

(20) Kim, R.; Kim, C.; Lee, S.; Kim, J.; Kim, I. W. *Cryst. Growth Des.* **2009**, *9*, 4584–4587.

(21) Perdikouri, C.; Putnis, C. V.; Kasiotas, A.; Putnis, A. *Cryst. Growth Des.* **2009**, *9*, 4344–4350.

(22) Pina, C. M.; Merkel, C.; Jordan, G. *Cryst. Growth Des.* **2009**, *9*, 4084–4090.

(23) Ruiz-Agudo, E.; Putnis, C. V.; Jimenez-Lopez, C.; Rodriguez-Navarro, C. *Geochim. Cosmochim. Acta* **2009**, *73*, 3201–3217.

(24) Henriksen, K.; Stipp, S. L. S. *Cryst. Growth Des.* **2009**, *9*, 2088–2097.

(25) Rohl, A. L.; Wright, K.; Gale, J. D. *Am. Mineral.* **2003**, *88*, 921–925.

(26) Deer, W. A.; Howie, R. A.; Zussman, J. *An introduction to the rock forming minerals*; Pearson Education Limited: Harlow, U.K., 1992.

*Corresponding author. E-mail: kuehnle@uni-mainz.de.

(1) Addadi, L.; Weiner, S. *Angew. Chem., Int. Ed. Engl.* **1992**, *31*, 153–169.

(2) Orme, C. A.; Noy, A.; Wierzbicki, A.; McBride, M. T.; Grantham, M.; Teng, H. H.; Dove, P. M.; DeYoreo, J. J. *Nature* **2001**, *411*, 775–779.

(3) Hazen, R. M.; Filley, T. R.; Goodfriend, G. A. *Proc. Natl. Acad. Sci. U.S.A.* **2001**, *98*, 5487–5490.

(4) Tucker, M. E.; Wright, V. P., *Carbonate Sedimentology*. Blackwell Scientific Publications: Oxford, 1990.

(5) Cölfen, H. *Curr. Opin. Colloid Interface Sci.* **2003**, *8*, 23–31.

(6) Hlubina, P.; Urbanczyk, W. *Meas. Sci. Technol.* **2005**, *16*, 1267–1271.

(7) Rieger, J.; Thieme, J.; Schmidt, C. *Langmuir* **2000**, *16*, 8300–8305.

(8) Hadicke, E.; Rieger, J.; Rau, I. U.; Boeckh, D. *Phys. Chem. Chem. Phys.* **1999**, *1*(17), 3891–3898.

(9) Stipp, S. L.; Hochella, M. F. *Geochim. Cosmochim. Acta* **1991**, *55*, 1723–1736.

(10) Hillner, P. E.; Manne, S.; Gratz, A. J.; Hansma, P. K. *Ultramicroscopy* **1992**, *42*, 1387–1393.

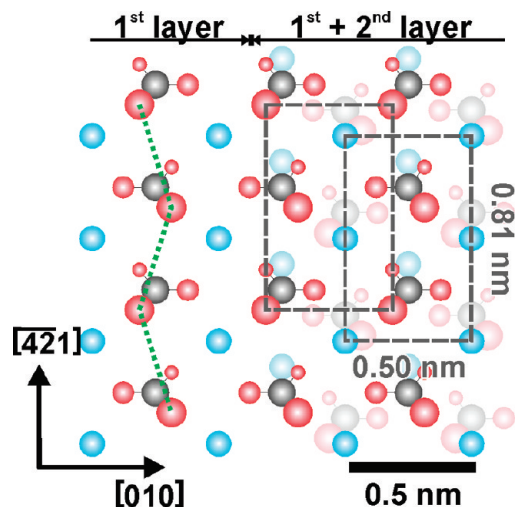


Figure 1. Calcite ($10\bar{1}4$) surface. Blue, red and gray circles represent calcium, oxygen and carbon atoms, respectively. The carbonate groups are tilted with respect to the plane, which is represented by different sizes of the oxygen atoms. In the right part of the figure, the second layer underneath is additionally shown. The two rectangles illustrate two different surface unit cells, the dotted line illustrates the characteristic zigzag structure of the protruding oxygen atoms.

a rhombohedral as well as hexagonal unit cell. The truncated bulk structure of the ($10\bar{1}4$) cleavage plane (referred to the hexagonal system) is shown in Figure 1. To the left, only the topmost layer is shown for simplicity, while to the right, we additionally display the second layer underneath to illustrate the relative orientation of the carbonate groups in the second layer. Within the ($10\bar{1}4$) plane, both calcium ions and carbonate groups form rectangular sublattices. The carbonate groups are tilted by 44.6° with respect to the ($10\bar{1}4$) plane such that one of the three oxygen atoms lies within the plane, one is above and one below the plane. Two possible unit cells having dimensions of $a = 0.50$ nm and $b = 0.81$ nm are marked in Figure 1.²⁷ As indicated by the dotted line, the protruding oxygen atoms form a zigzag structure along the $[\bar{4}21]$ direction. This is due to the fact that two inequivalent carbonate groups exist within the unit cell, rotated with respect to each other by 180° around an axis through the carbon atom normal to the surface plane. Thus, AFM images exhibiting a zigzag structure are usually ascribed to imaging the protruding oxygen atoms.^{12–18} However, considering the truncated bulk structure, the calculated amplitude of the protruding oxygen atoms in $[010]$ direction normal to the line connecting the carbon atoms amounts to ~ 0.064 nm, considering a C–O distance of $0.12867(6)$ nm (measured by X-ray diffraction).²⁸ Interestingly, in previous AFM experiments, the lateral deviation of the zigzag chain has been reported to vary from 0.07 to 0.21 nm, which corresponds to a zigzag amplitude of 0.035 to 0.105 nm.¹⁴

Besides the zigzag structure ascribed to protruding oxygen atoms, a rectangular structure with half the lattice spacing in $[\bar{4}21]$ direction (i.e., dimensions of $a' = 0.50$ nm and $b' = 0.40$ nm) has been observed using AFM in contact as well as in frequency modulation mode in liquids.^{10,17} Such a contrast can be understood when ascribing the imaged features to the calcium ions instead of the protruding oxygen atoms, which can be explained by a change in the tip termination.¹⁷

Most of the studies performed so far using contact and noncontact mode AFM reveal the characteristic zigzag pattern of the protruding oxygen atoms.^{12–18} Compared to the bulk-truncated structure, however, several deviations have been observed in many AFM measurements. First, as already indicated above, the observed zigzag amplitude varies compared to the expected value based on the unreconstructed model. Second, a phenomenon referred to as “row pairing” has been described in the literature,^{12,16,18} where every second protruding oxygen atom is imaged brighter along the $[\bar{4}21]$ direction, resulting in an apparent “pairing” of these species.²⁹ A tentative explanation for the row pairing has been given based on an inward-rotation of every second protruding oxygen atom along the $[\bar{4}21]$ direction.¹² From the apparent height difference of 0.6 nm, Jin et al. have determined a rotation of $35.4 \pm 5.2^\circ$.¹² It is, indeed, conceivable that the two carbonate groups rotate differently as they are inequivalent. Such a rotation would result in a lateral change in position by ~ 0.03 nm, which is, however, challenging to detect by AFM.

Third, both experimental and theoretical studies exist, reporting on an additional modulation along the $[010]$ direction, resulting in a (2×1) reconstruction. First experimental indication for a (2×1) reconstruction has been observed by Stipp et al. using LEED.⁹ Later, the (2×1) reconstruction has directly been revealed by the same group using contact mode AFM in liquids.¹⁸ However, similar AFM studies by other groups did not reveal this reconstruction, prompting a debate in literature whether the (2×1) reconstruction is a true surface property. A possible explanation of the contradiction was given by Stipp et al. proposing an adsorbate-induced effect.⁹ Moreover, a rotation of the carbonate groups has been discussed as a possible origin for the (2×1) reconstruction. However, the carbonate groups are equivalent along the $[010]$ direction, therefore, it appears unclear why adjacent carbonate groups should rotate in a different manner. A theoretical study has ascribed this discrepancy to the presence of an imaginary phonon mode.²⁵ The experimental validation for this is, however, still lacking.

Thus, it remains unclear so far (i) whether the (2×1) reconstruction is a true surface property and not just a measurement artifact and (ii) why it has been observed in several AFM studies and not in others.

Here, we present noncontact AFM measurements taken under ultrahigh vacuum (UHV) conditions both at room temperature and at 110 K. Performing the experiments in UHV allows for minimizing the influence of the surrounding environment. This is important when discussing whether the (2×1) reconstruction is adsorbate induced or not. Our atomically resolved images reveal a clear signature for a (2×1) reconstruction. The (2×1) reconstruction is visible in very narrow tip–surface distance ranges only, explaining the ongoing controversy whether the (2×1) reconstruction exists or not.

Experimental Details

All experiments are carried out under UHV conditions (base pressure $\leq 1 \times 10^{-10}$ mbar) using a VT AFM 25 atomic force microscope (Omicron, Taunusstein, Germany) operated in the frequency modulation noncontact mode (NC-AFM). The system is equipped with an easyPLL Plus phase-locked loop detector and amplitude controller (Nanosurf, Liestal, Switzerland) for signal demodulation and oscillation excitation. For experiments at

(27) Reeder, R. J. *Carbonates: Mineralogy and Chemistry*; Mineralogical Society of America: Washington, DC, 1983; Vol. 11.

(28) Effenberger, H.; Mereiter, K.; Zeemann, J. Z. *Kristallogr.* **1981**, *156*, 233–243.

(29) Note that the row pairing does not change the unit cell dimensions. Moreover, the term “pairing” might suggest a change in lateral position. However, within the uncertainty of the experiments, a lateral change has not been observed so far.

temperatures lower than room temperature a KONTI cryostat (CryoVac Gesellschaft für Tieftemperatur mbH & Co. KG, Troisdorf, Germany) is used.

For NC-AFM measurements we use n-doped silicon cantilevers (NanoWorld, Neuchâtel, Switzerland) with a resonance frequency of about 300 kHz (type PPP-NCH) operated with an amplitude of about 10 nm. Prior to their use, the cantilevers were Ar⁺ sputtered at 2 keV for 5 min to remove contaminants. In NC-AFM, a sharp tip mounted at the end of a cantilever is scanned over the surface, while the cantilever is driven at its actual resonance frequency. Because of tip–surface interactions, the resonance frequency changes, which is monitored as a resonance frequency shift Δf . When imaging in the constant height mode, Δf is recorded and displayed as a frequency shift image. When imaging in the constant frequency shift mode, Δf is kept constant by regulating the tip–surface distance. For all measurements reported here, the distance feedback loop was set very slow, yielding quasi constant-height images while still following the overall tilt of the sample surface; i.e., the presented images show Δf as a function of the tip position. All images are taken with a scanning speed of one line per second and 500 pixels per line. Fast and slow scan directions are indicated by the arrows in the upper right corner in each image. The images are displayed such that bright correspond to a highly attractive interaction while dark corresponds to less attractive or even repulsive interactions.³⁰ All images were corrected for thermal drift using the software tool SPIP (Image Metrology A/S, Hørsholm, Denmark).

Optical quality calcite samples from Korth Kristalle GmbH (Kiel, Germany) are cleaved in UHV, using a scalpel to score a line parallel to the edge of the crystal, resulting in flat (10 $\bar{1}$ 4) cleavage planes.³¹ Right after cleavage, the crystals are heated to 480 K for 1 h to remove surface charges.³² For experiments between 110 K and room temperature, the sample is cooled with liquid nitrogen. To reduce thermal drift, we usually wait for 2 h after attaching the cooling copper block to the sample before acquiring the first image. Note that the sample only is connected to the cryostat, the rest of the microscope remains at a temperature near room temperature.

Results and Discussion

In Figure 2, two typical images acquired in the quasi-constant height mode at room temperature are shown. In part a, an atomic-scale defect is shown (marked by a circle), demonstrating atomic-resolution imaging. For both images two possible unit cells are indicated by white rectangles. The lattice directions [010] and $[\bar{4}21]$ can be identified by the unit cell dimensions. From these dimensions alone it remains unclear whether the carbonate groups or the calcium atoms are imaged bright. However, the bright features form a zigzag line along the $[\bar{4}21]$ direction (indicated by zigzag lines in the images in Figure 2), suggesting that the protruding oxygen atoms of the carbonate groups are imaged bright. Similar to what has been observed in literature before, we observe different zigzag amplitudes. For the image shown in Figure 2a, the zigzag amplitude is about 0.1 nm. The image shown in Figure 2b is taken at another day with a different tip and, therefore, different tip conditions. In this image, a considerably larger zigzag amplitude of about 0.2 nm is observed.

Furthermore, when comparing the features along the $[\bar{4}21]$ direction, it is found that every second carbonate group is imaged brighter, representing the above-mentioned phenomenon of “row pairing” (indicated by orange ellipses). Note that no (2 × 1) reconstruction is visible in the images shown in Figure 2.

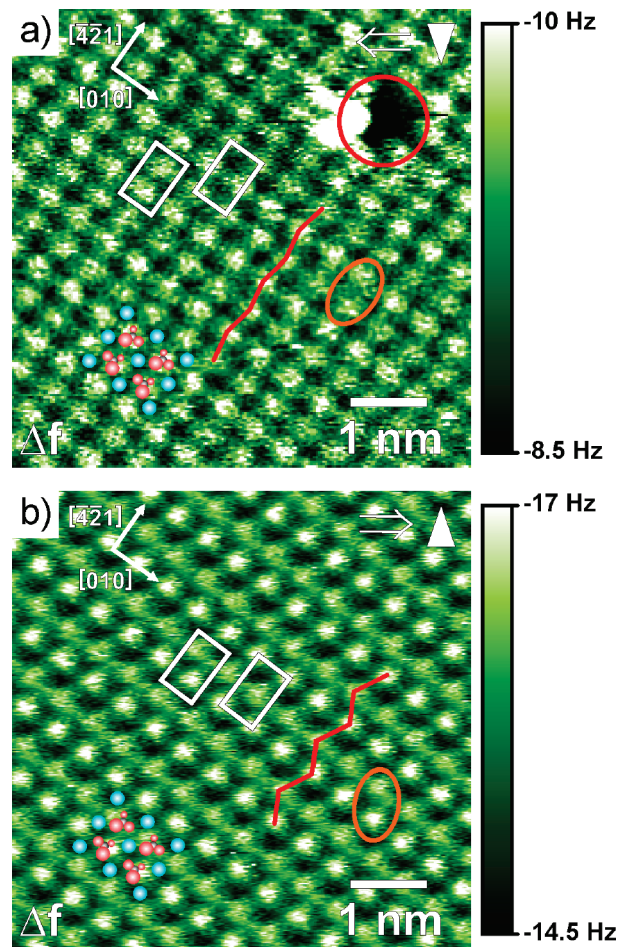


Figure 2. (a) Quasi-constant height image of the (10 $\bar{1}$ 4) calcite cleavage plane acquired at room temperature. An atomic-size defect (circle) demonstrates true atomic resolution imaging. Surface unit cells are marked by white rectangles. The alignment of the bright features along the $[\bar{4}21]$ direction is indicated by a zigzag line, showing an amplitude of about 0.1 nm. The different appearance of the features along the $[\bar{4}21]$ direction results in the so-called “row-pairing” as indicated by orange ellipses. (b) Image taken with a different tip and therefore different tip–sample interaction showing a much more pronounced zigzag structure with an amplitude of about 0.2 nm. $\langle\Delta f\rangle$ in part a is -9.3 Hz, and in part b $\langle\Delta f\rangle$ is -15.9 Hz.

However, a (2 × 1) reconstruction is observed depending on the tip–sample distance. In Figure 3, a series of four consecutive downward images is shown. Every 50 fast-scan lines the tip–sample distance is decreased by decreasing the average resonance frequency shift, $\langle\Delta f\rangle$. For large distances ($\langle\Delta f\rangle$ between -12 and -14 Hz) a (2 × 1) reconstruction is clearly visible as a modulation in [010] direction of the intensity of the dark lines between the bright imaged carbonate groups. Upon decreasing the tip–sample distance, the (2 × 1) reconstruction disappears (in a $\langle\Delta f\rangle$ -range between -15 and -18 Hz). When further decreasing the tip–surface distance ($\langle\Delta f\rangle$ between -19 and -26 Hz) the (2 × 1) reconstruction is visible again. We have repeated such distance-depended imaging series with different tips and different sample preparations. The observed change in appearance is reversible and reproducible as long as the tip remains stable.

Thus, for both large and small tip–sample distances the (2 × 1) reconstruction is visible as a modulation in the intensity of the dark lines, while for intermediate distances the (2 × 1) reconstruction is not visible. This behavior can be understood when

(30) Rahe, P.; Bechstein, R.; Schütte, J.; Ostendorf, F.; Kühnle, A. *Phys. Rev. B* **2008**, *77*, 195410.

(31) Tröger, L.; Schütte, J.; Ostendorf, F.; Kühnle, A.; Reichling, M. *Rev. Sci. Instrum.* **2009**, *80*, 063703.

(32) Wollbrandt, J.; Linke, W.; Brückner, U. *Exp. Tech. Phys.* **1975**, *23*, 65.

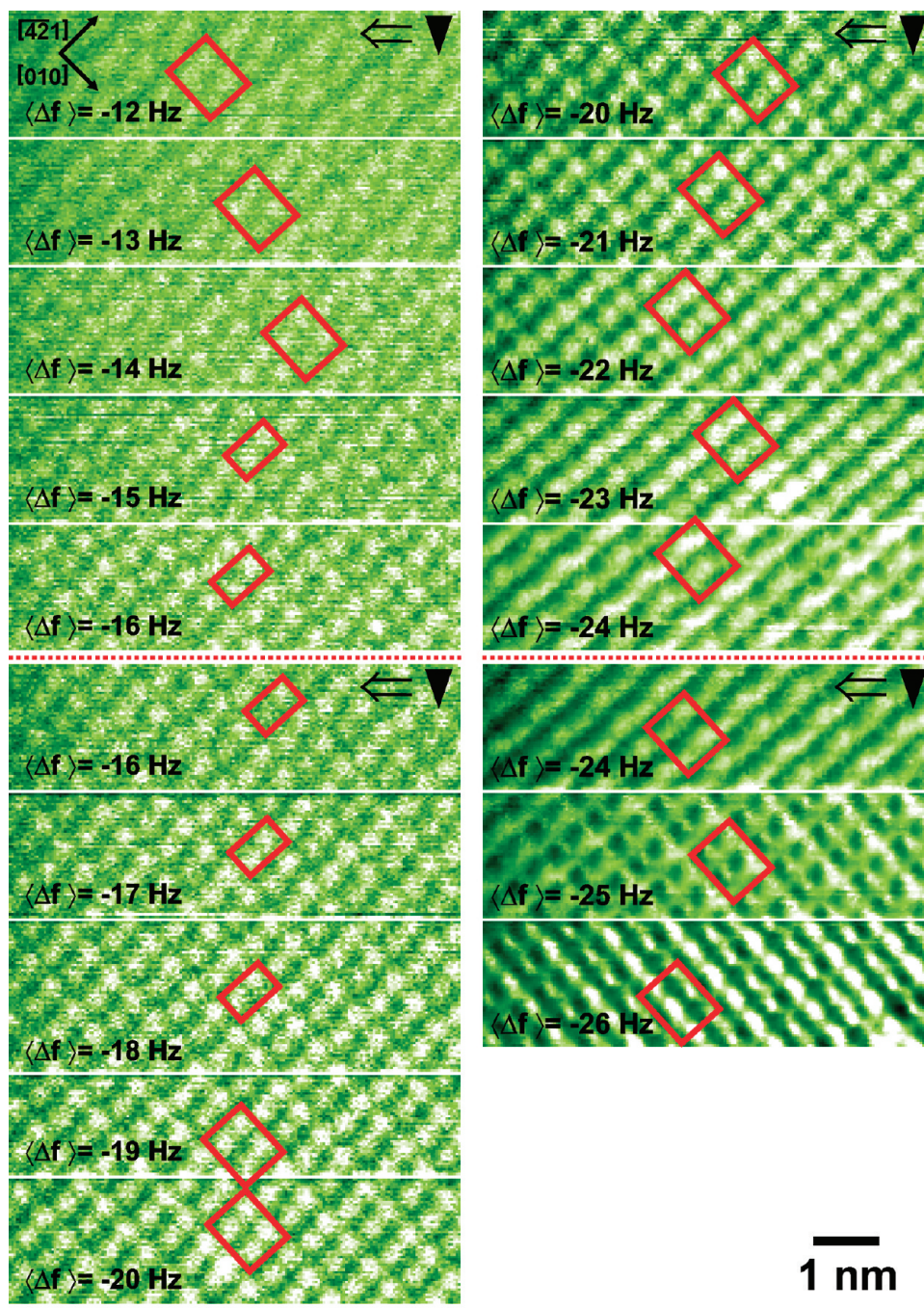


Figure 3. Four consecutive quasi-constant height images taken at room temperature where the tip–sample distance was stepwise reduced by decreasing $\langle \Delta f \rangle$. All images are taken with the slow scanning direction downward and the fast scanning direction from right to left. Apart from starting a new image (indicated by the red dotted lines), $\langle \Delta f \rangle$ is decreased by ~ 1 Hz every 50 fast scan lines. For large tip–sample distances ($\langle \Delta f \rangle$ corresponding to -12 to -14 Hz) and hence small tip–sample interactions the (2×1) reconstruction is strongly visible (indicated by the red rectangles). Upon decreasing the tip–sample distance and, hence, increasing the tip–sample interaction, the (2×1) reconstruction disappears. For $\langle \Delta f \rangle$ set points between -15 and -18 Hz the (2×1) reconstruction disappears, while it starts reappearing for set points between -19 and -26 Hz. Note that the (2×1) reconstruction is visible as a modulation in $[010]$ direction of the *dark* imaged lines between the bright carbonate groups, meaning every second dark line is imaged darker than the neighboring one (e.g., for -12 to -15 Hz, -21 and -22 Hz). In some cases, the (2×1) reconstruction becomes also apparent as modulation in $[010]$ direction on the *bright* carbonate groups, meaning every second carbonate group is imaged brighter than the neighboring one (e.g., for -23 to -25 Hz). The color scale for all images is adjusted such that the entire color scale from bright to dark is spanned over a range from $\langle \Delta f \rangle - 0.5$ Hz (bright) to $\langle \Delta f \rangle + 2.5$ Hz (dark).

considering the change of the resonance frequency shift as a function of tip–surface distance, $\Delta f(z)$.³³

(33) A detailed explanation including exemplary Δf versus distance curves are available free of charge via the Internet at <http://pubs.acs.org>.

The fact that the (2×1) reconstruction is observed only for some tip–sample distances prompts the question, whether this reconstruction is a true surface property or just induced by the tip.

If the (2×1) reconstruction is induced by the tip, we would anticipate that the reconstruction is more prominent for smaller

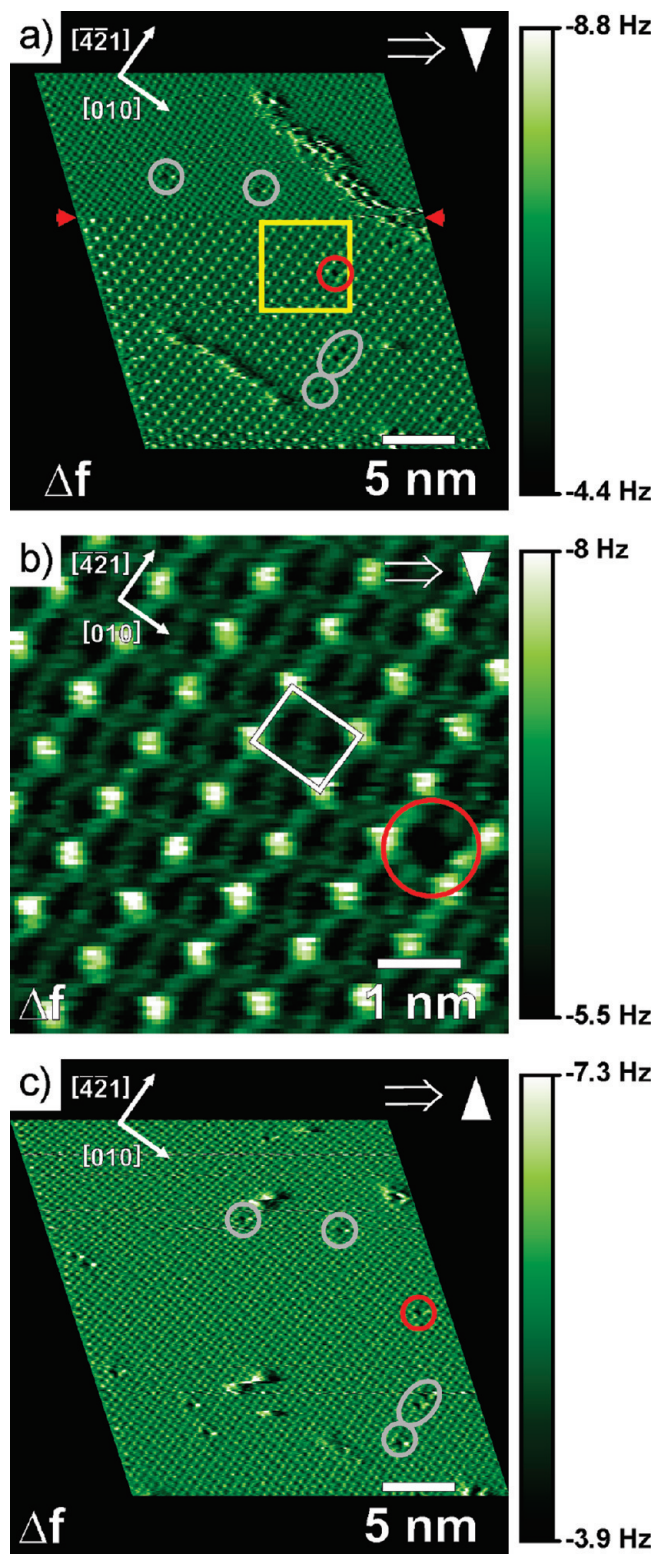


Figure 4. Consecutive quasi-constant height images taken at a sample temperature of 110 K. a) Downward image showing a tip change (marked by the red arrows) with simultaneous change in contrast taken at a $\langle\Delta f\rangle$ of -6.3 Hz. While in the upper part a (2×1) reconstruction is barely visible, in the lower part the (2×1) reconstruction is much more pronounced. (b) Zoom into the lower part of the image given in Figure 4a with the (2×1) unit cell superimposed. (c) In the consecutive upward image, the imaging contrast has changed back again ($\langle\Delta f\rangle -5.6$ Hz).

tip–sample distances. In our measurements, however, the opposite is observed: the (2×1) is well pronounced for large tip–sample

distances while it disappears when approaching the tip toward the surface. Additionally, we note that all carbonate groups within a row along the $[010]$ direction point in the same direction and are, therefore, equivalent. As the relative orientation of the tip with respect to the sample and, thus, relative to each individual carbonate group is not changed during imaging, a tip-induced change of the carbonate group orientation needs, as a matter of principle, to be identical for all carbonate groups within a row along the $[010]$ direction. Thus, an *alternating* appearance of the carbonate groups along the $[010]$ direction cannot be tip-induced, and, in turn, the observed (2×1) reconstruction cannot be tip-induced. The interaction between tip and sample can only weaken or enhance an already existing (2×1) reconstruction. Consequently, we interpret the present results in a way that the observed (2×1) reconstruction is a true surface property. The image series given in Figure 3 demonstrates the distance-dependent nature of the (2×1) reconstruction imaging contrast. The fact that the (2×1) reconstruction is observed in limited tip–sample distances only might explain the ongoing debate in literature whether the (2×1) reconstruction exists or not. Moreover, as our experiments were performed after cleavage under excellent UHV conditions, it seems rather unlikely that water or other adsorbates induce the (2×1) reconstruction as has been speculated in literature.^{14,18}

Besides the distance-dependent, continuous changes in imaging contrast discussed so far, we also observed sudden tip changes that were accompanied by a distinct change in atomic contrast. An example for such a contrast change is given in Figure 4a, which was acquired at a sample temperature of 110 K. Several defects are observed in this image (marked by red and gray circles).³⁴ Moreover, adsorbates are observed that are dragged along the surface during scanning, resulting in manipulation patterns.³⁵ In the upper part of the image, a tip change has occurred and the atomic contrast changed dramatically. While in the upper part the (2×1) reconstruction is barely visible, a well pronounced (2×1) pattern is present in the lower part of the image. A zoom into this structure with a superimposed (2×1) unit cell is given in Figure 4b. In the consecutive upward scan (Figure 4c), the imaging contrast has changed again, revealing the same imaging contrast as observed in the upper part of Figure 4a. Note that the imaging position is the same as evidenced by the position of the atomic-size defects that serve as a landmark.

Conclusions

We present high-resolution NC-AFM images of the $(10\bar{1}4)$ cleavage plane of calcite taken under UHV conditions both at room temperature and at 110 K. Our images exhibit atomic-scale defects, demonstrating atomic resolution imaging. We frequently observe an alternate appearance of bright features along the $[421]$ direction, corresponding to the so-called “row pairing” previously described in literature. Moreover, depending on the tip–sample distance, a (2×1) reconstruction is revealed. This (2×1) reconstruction is visible in very narrow tip–surface distance ranges only, explaining the ongoing controversy in literature whether this reconstruction is a true surface property or not. As all images presented here are taken after cleavage and subsequent annealing in UHV, adsorbed water or other air-borne species are rather unlikely to be present on the surface. Consequently, adsorbed species are most unlikely to be the origin of the (2×1) reconstruction.

(34) These defects most likely result from adsorbing species from the residual gas.

(35) Hirth, S.; Ostendorf, F.; Reichling, M. *Nanotechnology* **2006**, *17*, S148–S154.

Moreover, as the relative orientation of the carbonate groups with respect to the tip is the same for all carbonate groups within a row along the [010] direction, the (2×1) reconstruction is not tip-induced either. In summary, all of our results suggest the (2×1) reconstruction to be a true surface property.

Acknowledgment. This work has been supported by the German Research Foundation (DFG) through the Emmy Noether program

(KU1980/1-2) and the Niedersachsen Ph.D. program “Synthesis and Characterisation of Surfaces and Interfaces assembled from Clusters and Molecules”.

Supporting Information Available: Figures showing exemplary Δf versus distance curves and experimental Δf versus Δf set point curves. This material is available free of charge via the Internet at <http://pubs.acs.org>.